MRI Brain Scans Classification Using Bi-directional Modified Gray Level Co-occurrence Matrix and Long Short-Term Memory

Marwah Hamad Hasan[1*], Hussain S. Hasan[2], Ali M. Hasan[3]

Abstract

Due to the large number of MRI slices provided for each patient, the MRI visual evaluation process of brain disease diagnosis has become time-consuming, slow and more vulnerable to error. In this research an algorithm is proposed to extract texture feature and classify MRI brain scans into normal and abnormal MRI scans. First, the MRI scans are pre- processed by image enhancement, intensity normalization and correcting the mid-sagittal plane (MSP) of brain. Second, the proposed bi-directional modified gray level co-occurrence matrix (Bi-MGLCM) method is used to extract texture features from MRI T2-weighted images that are used to measure the degree of symmetry between the left and right hemispheres of the brain. Finally, these features are classified into normal and abnormal by using long-short term memory (LSTM) model. The research will be validated using two datasets; a real dataset that was collected from the magnetic resonance imaging unit in Al-Imamain Al-Kadhimain Medical City – Baghdad - Iraq in 2019 and the standard data set for classification of brain tumors (BRATS 2013). The achieved classification accuracies were 96.3% for the collected dataset and 98.9 % for the BRATS 2013.

Key Words: Deep Learning, MGLCM, MRI Brain Scans, Feature Extraction, LSTM Classifier.

DOI Number: 10.14704/nq.2020.18.9.NQ20216 **NeuroQuantology 2020; 18(9):54-63**

Introduction

Medical imaging is a medical field branch that uses technology to take pictures of the internal organs of human body. medical imaging often refers to diagnostic imaging, especially as it is used to help doctors to be able to accurately diagnose (Birry, 2013). Therefore, the analysis of medical images specializing in the study of brain tumors has received attention in recent periods due to the need for an effective and objective evaluation of large amounts of data. However, the increasing approaches in the application of automated methods to analyze existing images of brain tumors go back to nearly two decades, but the current methods have become more mature and approach to what has to do with routine clinical application (Bauer, 2013). Indeed, the field of medical image processing has become especially important and plays a major role in clinical practice applications as biomedical imaging helps in the pathologies of patients diagnosed. Brain tumors are crucial cases in medical imaging as their accurate detection and segmentation influences clinical diagnosis considerably. They also help in predicting prognosis and treatment, as well as benefiting the general modeling of brain pathologies and their anatomical construction (Nabizadeh, 2015).

Corresponding author: Marwah Hamad Hasan
Address: [1,2,3]Department of Physiology and Medical Physics, College of Medicine, Al-Nahrain University, Baghdad, Iraq.
[1*]E-mail: alhidarymarwa@yahoo.com

Relevant conflicts of interest/financial disclosures: The authors declare that the research was conducted in the absence of any commercial or financial relationships that could be construed as a potential conflict of interest.
Received: 17 July 2020 **Accepted:** 16 August 2020

Which means that MRI is considered one of the most common medical imaging techniques, especially since such imaging will not be surgical and does not use any ionization radiation, besides it is able to display different tissue images with high accuracy and with good contrast. In addition, MRI works to produce multiple images from the same region in the tissue with different and different vision possibilities through different image capture protocols and parameters. Also, these images provide additional useful anatomical information regarding the tissue region, and thus the information provided will support researchers in the field of brain disease study in a more accurate and in-depth manner. But dealing with such images creates one of the most difficult problems, which is the separation of some cells and specific tissues from the rest of the image (Nabizadeh & Kubat, 2015). Finally, it must be clarified that imaging of human organs through the use of magnetic resonance imaging is the focus of many research projects, especially those related to specific types of tumors such as breast, lung, liver, and brain tumors. This has been demonstrated by the need to develop a system for examining and automating the fragmentation of brain tumors, as this mechanism will provide speed in extracting images. Thus, the general framework of the screening system will deal with a set of data and pre-processing and has many special advantages in choosing what is desired of the advantages and classifications. Therefore, in order to choose the most appropriate proposed methods in relation to the open system, a comprehensive review of all research conducted at different stages of diagnosis is made and the justification for doing these options has been clarified (Al-Waeli, 2017).

Related Work

Zulpe and Pawar (2012) used the gray common occurrence matrix (GLCM) method four different categories of brain tumors and their extraction Structural features based on each category, applied to bilayers forward feed of neural network, which gives 97.5% rating rate.

Similarly, (Lahmiri & Boukadoum, 2013) those who have developed a new method for the automatic features extracted from biomedical images and through the use of two-dimensional waves, namely DWT and Gabor with different directions and frequencies. The classification was execute using support vector machine (SVM) 50%, 68%, and 86% accuracy attain on retina mammograms, mammograms, and MRI brain scans, respectively.

Birry (2013) as determination of using of GLCM, along with discrete cosine transform (DCT), to extract the feature from 36 images. In this context, it must be clarified that there are many criteria used with traditional classification techniques, such as what is done in cross-linking, and Euclidean distance scales aimed at identifying tissues with experimental images. It is worth noting that the success rate in the traditional distance method using cross correlation is 68% to 70%.

Singh (2015) those who suggested a new technique based on the support vector (SVM) and fuzzy c-specialists in categorizing brain tumors, the intended algorithm represents a mixture of SVM and fuzzy c- which means there is a hybrid technology to predict if there is a tumor in the brain. Thus, the image is improved through the use of improvement techniques related to contrast and medium range. However, the use of Double skulls and morphology is of particular importance in the skull stripe. As for the fuzzy c- means (FCM) used to segment the assembly image in order to detect what is in the suspicious region of the brain's MRI image. However, the gray level run length matrix (GLRLM) is used to extract a feature in the brain image, and therefore SVM technology is applied in order to classify MRI images in the brain, because of its advantages lies in providing an accurate and more effective classification of MRI images of the brain.

Sachdeva, Kumar, Gupta, Khandelwal, and Ahuja (2016) developed a system that helps radiologists classify brain tumors. The proposed system consists of three main units; the first brain tumors are fragmented using a semi-automatic content-based active contour model (CBAC). Brain tumors are divided by using a semi-automatic content-based active contour model (CBAC). The second feature extraction was performed using GLCM, LoG, Gabor wavelet, RILBP, IBF and shape feature (SBF) after that, followed it the feature selection to measure the suitability of the features with GA. In the end, SVM and MLP were used to help classify brain tumors, but the results were compared with the results they found and in the performance of each of them, so that the accuracy achieved in the first tool was 91.7%, while the second was the achieved accuracy rate of 94.9%.

Shree and Kumar (2018) in this regard, a technique was proposed to remove the noise and extract the

properties of the gray-level joint matrix (GLCM), in order to detect existing tumors in the brain by relying on DWT. In that regard, the growth area is segmented to improve efficiency and reduce complexity. From this, the Morphology Filter will remove the noise that may form after fragmentation, and the experiment has obtained 100% accuracy in detecting existing natural and abnormal tissue.

Jalab and Hasan (2019) Those who proposed a special algorithm in extracting the characteristics of deep learning aimed at finding the modified gray-level co-occurrence matrix (GLCM) method, which are designed to extract the relevant features by carrying out brain scans. However, related features are combined with manual features in order to enhance brain classification operation through MRI and through the use of SVM as a classifier. However, the results of the study were obtained through a mixture of deep learning methodology and manual functions extracted through MGLCM, which increased accuracy to 99.30% of SVM accuracy.

The rest of the paper is organized as follows: Section 3 reviews some related state-of-art methods that have been proposed recently, provides the details of the proposed method of MRI brain tumors classification and presents the experimental results and finally, the conclusions are given in Section 4.

Materials and Methods

The main objective of this study is to build an automated algorithm that aims to classify MRI scans into regular and abnormal scans. This will also improve the diagnosis procedures' quality as clinicians can spend more time on patients on pathological brain. It starts with the data collection phase from the Iraqi hospital. A set of algorithms in the pre-processing stage are implemented and they are followed by a features extraction algorithms and classification.

1) Data Collection

The data collection stage is considered a basic stage in this study, and in this stage two sets of data were used. While the group of clinical pictures consists of 214 images of the brain were imaged through magnetic resonance imaging, and they were obtained through diagnostic procedures in the magnetic resonance imaging unit located in Al-Imamain Al-Kadhimain Medical City – Baghdad - Iraq. Clinicians operating in this unit had identified and categorized this data as normal and abnormal. This is done by using a SIEMENS MAGNETOM Avanto 1.5 Tesla scanner (USA), In addition to PHILIPS Achieva 1.5 Tesla scanner (Netherlands). The collected dataset includes 107 MRI scans with different pathologies and the rest without any detectable diseases. The brain scanning process with MRI has a high degree of difference in relation to the shape and location of the tumor, but they have less intensity variation and less artefact-loaded than real images to measure the algorithm's ability to deal with variation in the shape and location of brain tumors. Figure 1 shows some examples of real and standard data sets used in this study with different methods T2-w, FLAIR and T1c-w.

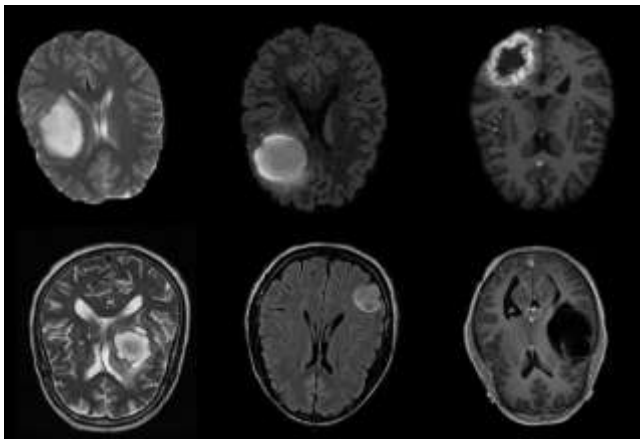

Figure 1. Examples from the used datasets: The collected dataset in the first row and the standard dataset in the second row

2) Image Preprocessing

The pre-processing step involves performing a group of algorithms on the MRI slide scans as a ready for the feature extraction stage such as unify MRI slice dimensions, intensity enhancement, normalizing the intensity of the MRI and MSP of brain detection and correction algorithm.

3) MSP Detection and Correction

progress in medical imaging technologies give facilities for the internal conception of the brain. Using these medical images, diagnosis and visual interpretation are made by clinicians. Method of determining MSP is an important first stage in analyzing the image of the brain because it provides a first estimate to evaluate brain diseases and discover tumors (Jayasuriya & Liew, 2012). The human brain is divided into two halves around

the MSP, with almost bilateral symmetry.
It means that certain structures on one side of the brain have an equivalent shape and location identical on the other side. The two hemispheres are divided by a longitudinal slit in the form of a membrane that divides the sphere into two equal halves right and left. This longitudinal fissure is full of with CSF and used to visually distinguish the two hemispheres (Ruppert, Teverovskiy, Yu, Falcao, & Liu, 2011). The separation of the two brain segments of the hemispheres in axial MRI was achieved by defining the MSP along the fissure used as a guideline for study of asymmetry. MSP for the brain is the same direction of the head of patient. Symmetry is significant indicator of its normality or abnormalities, so that general pathologies diseases like tumors, stroke, It is possible to determine the state of bleeding through similarities based on what is found in the analysis of images imaged with magnetic resonance MRI of the brain, which means that the growth of the ability of cancer cells breaks the similarity, especially with the MSP curve of the brain (Liu, Collins, & Rothfus, 1998). MSP extraction process can be sorted into two sets: methods based on content and methods based on shape (Ruppert et al., 2011). However, the content-based approach is based on trying to find a level for that increasing in the symmetrical measurement between brain sides (Ardekani, Kershaw, Braun, & Kanuo, 1997).
The main obstacle to the widespread adoption of these methods in actual neural implementation is hardness is the measurement of symmetry as well as determining the location of the MSP for the brain under the presence of abnormal conditions, for example air pockets and lesions must be neglected when counting the axis of similarity (Hu & Nowinski, 2003; Liu et al., 1998). Moreover, methods that based on shape use fissures between the hemisphere as a simple parameter to extract and discover MSP for the brain that indicates the level of symmetry (Bergo, Falcão, Yasuda, & Ruppert, 2008). In parallel axial slides, the incision lines between the two inner hemispheres are parallel to the direction of the head of patient (Hu & Nowinski, 2003). In this study, the focus was on knowing the patient's head direction instead of calculating symmetry in order to know the MSP of the brain, and it was relied on that to use the PCA method required to perform the calculation of the distinct principle axes that are perpendicular to each other. However, these axes are used to distinguish the patient's head by calculating the mass distributed entirely, while each plane is similar in the body perpendicular to the main axis (Al-Waeli, 2017).

4) Feature Extraction

a) Preparing MRI Brain Slices for Feature Extraction

This step involves implementing a group of image pre- processing algorithms to ready MRI brain slides and making them more appropriate to implement the MGLCM method. The inputs to this step are the MRI brain scan corrected and output contain only head of patient with dimensions (512 x 512) pixels. The MRI slices are cropped from the upper margin of the slices to the upper boundary of the skull. The same procedure is then used for cropping the MRI slices from the bottom margin of the slices to the bottom boundary of the skull. The left and right boundaries can be identified by measuring the distance between the upper and bottom boundaries. In fact, the left and right boundaries are away from the middle of the MRI slices which denotes the brain MSP by a half distance between the top and bottom boundaries s shown in figure 2. Finally, each cropped MRI brain slice is resized to (512 × 512) pixels, before using the MGLCM process.

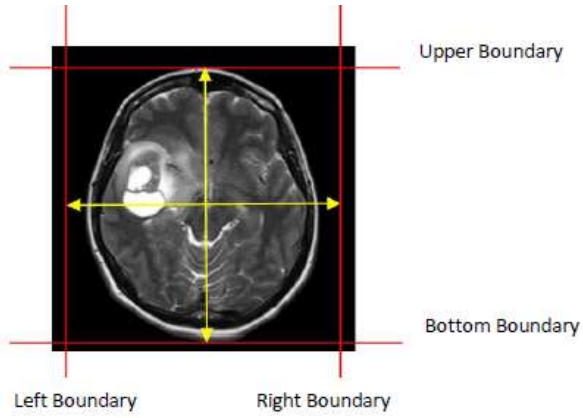

Figure 2. MRI brain slice cropping

b) Bi-directional Modified Grey Level Co-occurrence Matrix Method (Bi-MGLCM)

Bi-MGLCM suggests in this study, it is a second degree statistical method for generating textual features and providing information on the pattern scans textures of MRI. Use these features statistically to calculate the degree of similarity among the cerebral hemispheres, the normal state,

and abnormalities of human brain. Bi-MGLCM aims to create tissue properties by knowing and calculating the spatial relationship that binds the common frequencies of all pair combinations, in order to form a gray level for all pixels in the left and right hemispheres. It is worth noting that in the beginning, the left side of the brain is considered as a basic reference through which nine simultaneous matrices are extracted from the right half of the brain and this is done according to the following displacements θ = (45, 45), (0, 45), (315, 45), (45, 0), (0, 0), (315, 0), (45, 315), (0, 315), (315, 315), and one distance d=1. Then, the right hemisphere is considered as a reference and extract seven co-occurrence matrices form the left hemisphere of the brain under the same offsets expect ignoring θ = (0, 0) because this offset gives the same features that are extracted when considering the right side of the brain as a reference, as shown in figure 3. Thus, since nine and eight co-occurrence matrices are determined from left and right hemispheres respectively, 17 common matrices are obtained for each MRI scan. Then each synchronous matrix is normalized in order to calculate what is present in the relative frequency of the joint event between all the gray levels of the connected pixels between both halves of the cerebral sphere, and this is done by the total number of all elements.

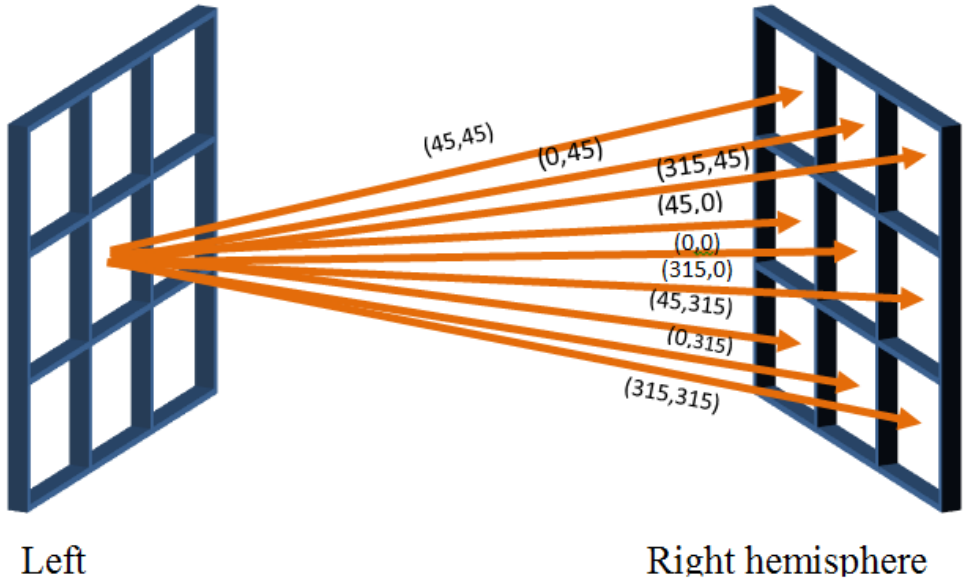

Figure 3. How reference pixel in the left side of brain, relates with opposite nine pixels in the right hemisphere

When, the left hemisphere is considered as a reference, the Bi-MGLCM is determined by using Eq. 1.

$$P(i,j)_{(\theta_1,\theta_2)} = \frac{1}{256^2}\sum_{x=1}^{512}\sum_{y=1}^{256}\begin{cases}1 & ,if\ L(x,y)=i\ and\ R(x+\Delta x,y+\Delta y)\\ 0 & ,Otherwise\end{cases} \quad (1)$$

While, when the right hemisphere is considered as a reference, the Bi-MGLCM is determined by using Eq. 2.

$$P(i,j)_{(\theta_1,\theta_2)} = \frac{1}{256^2}\sum_{x=1}^{512}\sum_{y=1}^{256}\begin{cases}1 & ,if\ R(x,y)=i\ and\ L(x+\Delta x,y+\Delta y)\\ 0 & ,Otherwise\end{cases} \quad (2)$$

Where, L and R denote the left and right hemispheres, respectively. Each of them has a pixel size that is calculated by the following formula: (512 x 256). However, P represents the matrix produced by the concurrent event, and i and j are the coordinates of the concurrent matrix. As for the values of Δx and Δy, they depend on the direction of the measured matrix and this is done by relying on the following rules:

If θ_1= 0 and θ_2= 0 then Δx=0 and Δy=0,
If θ_1= 0 and θ_2= 45 then Δx=-1 and Δy=0
If θ_1= 0 and θ_2= 315 then Δx=1 and Δy=0,
If θ_1= 45 and θ_2= 0 then Δx=0 and Δy=1,
If θ_1= 315 and θ_2=0 then Δx=0 and Δy=-1,
If θ_1= 45 and θ_2= 45 then Δx=-1 and Δy=1,
If θ_1= 315 and θ_2= 45 then Δx=-1 and Δy=-1

The co-occurrence and resultant matrices are somewhat similar to what exists in the normal brain in terms of the diameter of the anterior matrix, when the minds are abnormal and asymmetric. This is shown in figure 4, and what it shows in the shape of the brain that was imaged natural and abnormal magnetic resonance and this is shown by scanning the corresponding synchronization matrix in the angles θ1 = 0 and θ2=2 = 0. On the left side, there is an MRI scan and

a cross-occurrence matrix of the normal brain scan. It is worth noting that the MRI scan of the average patient appears as if the two hemispheres of the brain are identical around the MSP, and also the corresponding correlation matrix appears as if it were narrower with the symmetry side around the forward diameter. While on the right is the MRI scan and corresponding co-occurrence matrix of an abnormal brain scan. The patient has a tumor in left hemisphere of his brain, and it makes his brain asymmetry around MSP. Again, the corresponding co-occurrence matrix is Much wider and asymmetry around the forward diagonal. 17 concurrent matrices have been assigned after the modified and bi-directional gray common frequency matrix has been applied, in addition to that 21 statistical descriptions have been identified for each concurrent matrix; That is, there are 357 descriptions of each brain slice imaged through MRI. Besides, the cross-correlation was described once for each MRI segment. Finally, approximately 358 descriptions of each segment of the brain that were imaged with MRI were extracted, while the workbook uses these features to distinguish between MRI scans, to distinguish between normal and abnormal tissue.

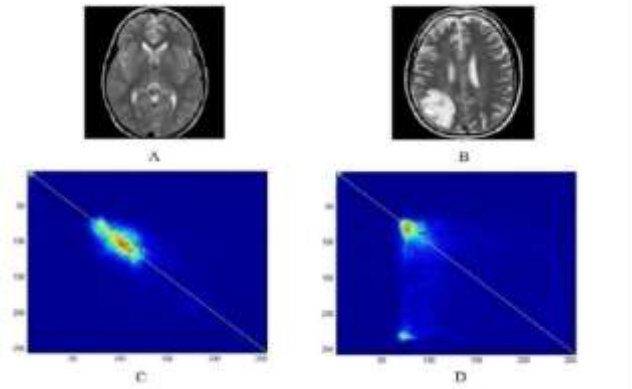

Figure 4. A) MRI normal brain slice, B) MRI abnormal brain slice, C) MGLCM of normal brain scanning and D) MGLCM of abnormal brain scanning

5) Feature Selection

It is possible for the high-dimensional feature groups to negatively affect the classification results, as there are many advantages that can reduce the accuracy of the classification due to the presence of repetition or lack of relevance to some features. One of the main goals of feature selection technologies is to try to define a small subset of features that reduce the increase and increase the relevance (Al-Waeli, 2017). The selection of the feature is therefore an significant step in uncovering the most useful features and in improving the efficiency of the classifier to categorize anonymous data reliably (Pantelis, 2010). The main function of ANOVA is to measure the importance of the feature as it is considered a powerful statistical technique by which to analyze data and discover the importance of the predictive tool contained within the feature. It is worth noting that setting the critical value α to 0.001 aims to get very large missions (Johnson & Synovec, 2002). because the value of P lower than 0.001 is not enough to measure the predictor's significance. Instead of that, the predictor most has a height statistical value. The rise statistical value of F shows that classes are largely separate from one another (Hasan & Meziane, 2016).

Table 1. shows an explanation of the differences in the advantages of MRI groups for both normal and abnormal brain tissue, and for brain scans of the presence matrix at θ1 = 0 and θ2 = 0. ANOVA was performed using IBM SPSS statistics version 20 (Al-Waeli, 2017). This means that ANOVA works to reduce the number of descriptors from 358 to 204, and in that 12 important features were selected for each segment of the brain that was imaged. These features are: contrast, cluster prominence, cluster shade, dissimilarity, entropy, sum of square variance, sum average, sum variance, sum entropy, difference energy, weighted distance in addition to the cross correlation. In figure 5, it shows the great difference between the average of these recipes for both major groups.

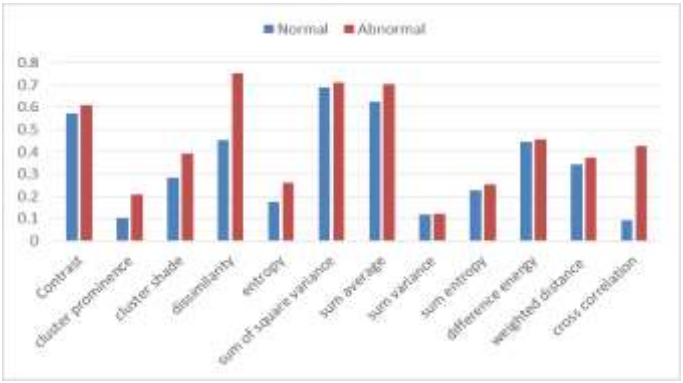

Figure 5. Means of the extracted and selected Textural features of the normal and pathological MRI brain scans

However, there is a difference in the ranges that exist for the extracted descriptors, and this is what works to find many of the descriptors that have large values and of course it has a greater effect than the effect that descriptors with small values do on the classifier method (Larose & Larose, 2014).

Data normalization is a basic step in preparing and normalizes given descriptors to standardize the effect of each descriptor. It assist to improve the performance of the classifier by converting the given prescriptions to a preferable and more appropriate form of the training process (Jayalakshmi & Santhakumaran, 2011).

In this study, the min-max normalization path was used to perform the linear transformation of the extracted recipes, in addition to maintaining the existing relationships between the original descriptors.

Table 1. Comparison of MRI brain scans feature (mean ± standard deviation (SD)) between normal and abnormal patients

Features	Abnormal MRI scans	Normal MRI scans	F-statistic	P-value
Auto correlation ($\times 10^3$)	6.11±1.07	5.71±1.66	5.831	0.016
Contrast ($\times 10^3$)	2.1±0.69	1.04±0.41	233.16	<0.001
Correlation (÷10)	7.04±0.92	8.05±0.85	3.4	0.066
Cluster Prominence ($\times 10^8$)	3.92±2.05	2.84±1.07	28.56	<0.001
Cluster Shade ($\times 10^5$)	7.52±5.28	4.54±3.39	30.12	<0.001
Dissimilarity (×10)	2.6±0.55	1.73±0.35	234.7	<0.001
Energy (÷100)	9.57±2.27	9.79±2.65	2.7	0.075
Entropy	7.13±0.34	6.91±0.37	21.03	<0.001
Homogeneity (÷10)	3.44±0.39	3.62±0.39	2.1	0.098
Max. Probability (÷10)	3.07±0.38	3.1±0.42	1.7	0.13
Sum of Square Variance ($\times 10^3$)	7.03±1.43	6.27±1.67	16.84	<0.001
Sum Average ($\times 10^2$)	1.22±0.11	1.16±0.19	9.788	0.002
Sum Variance ($\times 10^4$)	2.55±0.43	2.29±0.64	16.23	<0.001
Sum Entropy	4.56±0.18	4.45±0.21	9.1	0.003
Difference Entropy	3.73±0.22	3.43±0.2	92.07	<0.001
Information Measure of Correlation I (÷10)	2.19±0.32	2.48±0.29	2.65	0.79
Information Measure of Correlation II (÷10)	9.1±0.22	9.25±0.19	2.2	0.091
Inverse Difference Normalized (÷10)	9.21±0.15	9.44±0.1	1.75	0.11
Inverse Difference Moment Normalized (÷10)	9.73±0.08	9.86±0.05	2.53	0.084
Weighted Mean	1.19±0.81	0.32±0.17	2.85	0.071
Weighted Distance	4.25±3.31	0.9±0.72	116.5	<0.001
Cross Correlation (÷10)	8±0.85	7±0.9	3.4	0.066

6) Feature Classification

In this study there are two classes; the positive class refers to the pathological brain scans and the negative class refers to the normal brain scans. the collected dataset in this study includes MRI brain scans of 214 cases and it was Clinically classified by physicians as natural and abnormal. The highest precision in classification with the best results was obtained using the LSTM network at 96.3 %. The performance of LSTM network is compared with the achieved accuracy of other classifiers such as SVM, Naïve Bayes and KNN, as demonstrated in table 2. These results prove the superiority of LSTM network to classify MRI brain scans precisely.

Table 2. The comparison of performance for several networks with the achieved accuracy of other classifiers

Method	Accuracy 100%	TP 100%	TN 100%
Quadratic SVM	93%	96.2%	89.7%
Naïve Bayes	92.5%	94.4%	90.6%
KNN	92.1%	97.2%	86.9%
LSTM	96.30%	98.1%	94.4%

The LSTM requires to be configured by setting the parameters of network optimally. These configuration parameters are configured experimentally by trial and observe the performance and the optimal parameters that gave high classification accuracy. In this study, the LSTM network includes 7 layers; sequence input with 204 dimensions that comes from the extracted features of each MRI brain scan, LSTM with bidirectional LSTM layer (Bi-LSTM) with 500 hidden units, two fully connected layers, soft max classifier and classification output layers. Additionally, the LSTM network was trained by using Adam optimization method, maximum Epoch value was set to 700 and gradient threshold value was set to 1. Figures 6, and 7 shows the flowchart and steps and how the training process of LSTM network is directly proportional with the number of iterations respectively.

In this study, a set of data called BRATS 2013 was applied, with the aim of estimating the proposed algorithm (Menze et al., 2014). There were approximately 25 surveys performed through magnetic resonance imaging, as well as working to change the shape, location and severity of the tumor. It is worth noting that the data that were found was classified through the use of the existing and proposed algorithm because of its high

accuracy reached 98.9%, besides that there was a comparison between the experimental results of the proposed algorithm and what indicated by previous studies that were clarified in table 3.(Hasan & Meziane, 2016).

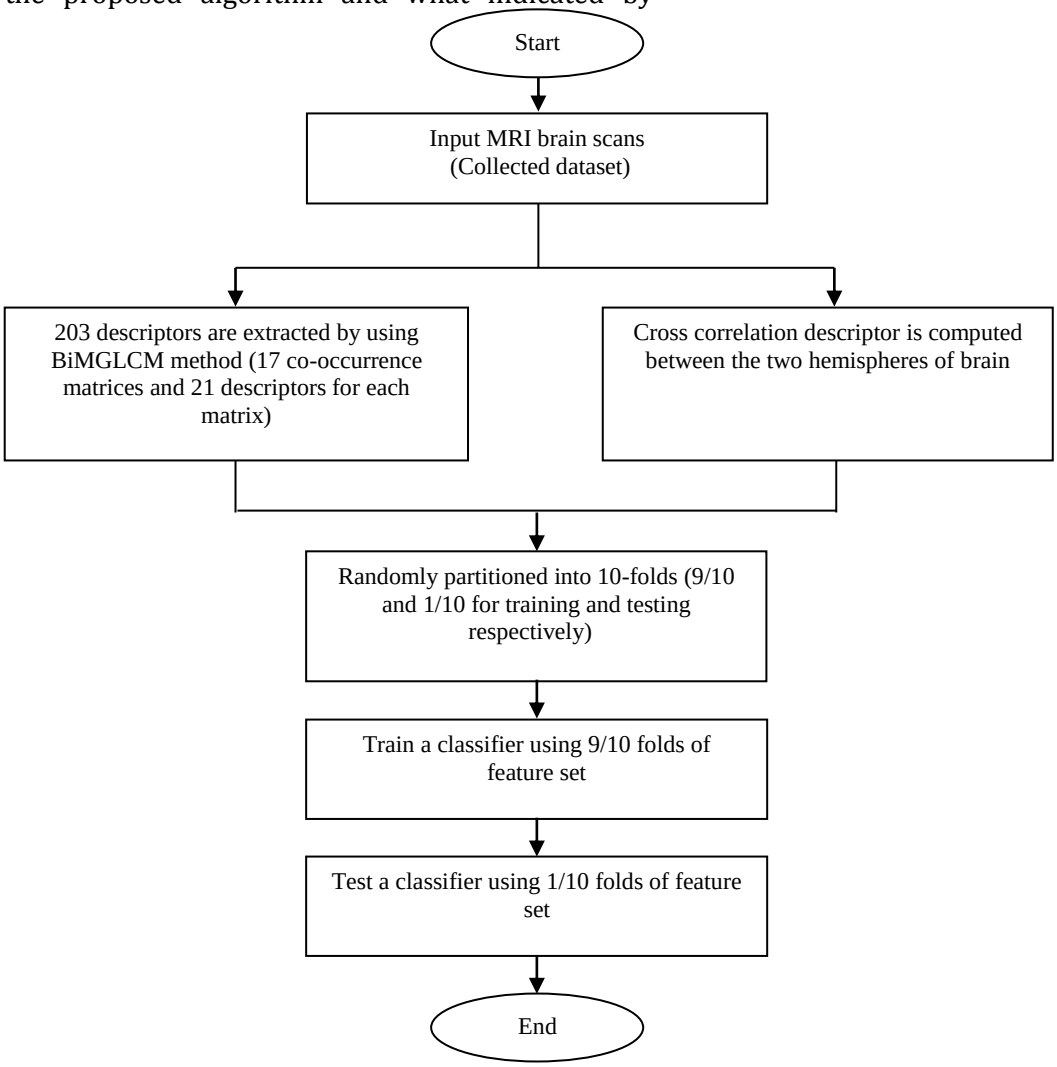

Figure 6. Flowchart and steps of training and testing of classification techniques

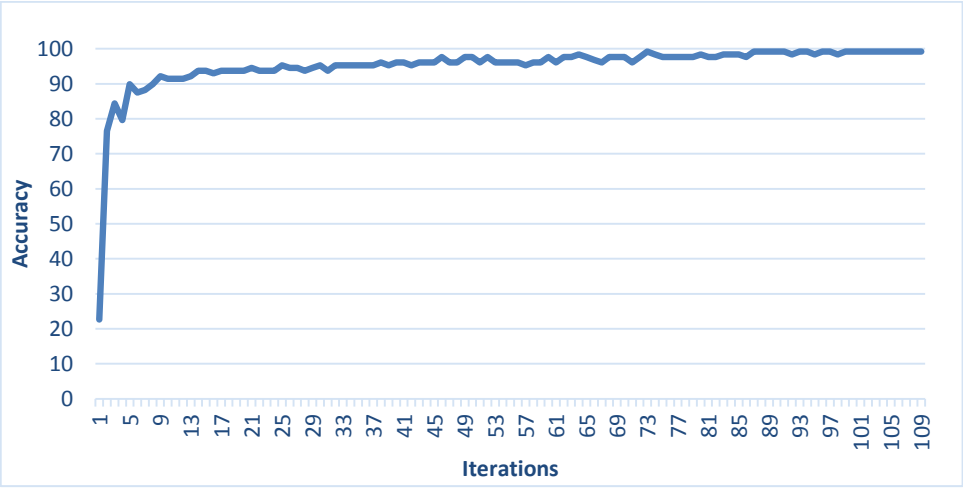

Figure 7. The training process of the LSTM network

Conclusion

It must be clarified that the visual diagnosis that is done through the use of MRI is considered a personal diagnosis and that it is based on the expertise of the radiologist, and for this was studied tissue analysis in order to develop the diagnostic process that is carried out through the use of MRI images. In this study, there were approximately 12 statistic events that were selected by ANOVA as an important feature, and through the presence of seventeen BiMGLCM matrices that are used to distinguish existing abnormalities in brain tissue.

Table 3. Comparison for previous suggested methods

Reference	Features methods	No. of Patients	Classifier	Accuracy
Nabizadeh (2015), Nabizadeh and Kubat (2015)	- First-order statistical - GLCM (4 orientations and 2 distances) - GLRLM (4 orientations) - HOG - LBP	25 (BRATS 2013)	SVM	97.4%
Gómez, Pereira, and Infantosi (2012)	GLCM (4 orientations and 10 distances)	436	LDA	87%
Sachdeva et al. (2016)	- GLCM (4 orientations and 1 distances) - LoG - DGTF - RICGF - RILBP - IBF - SBF	55	SVM	91.7%
			MLP	94.9%
(Hasan and Meziane (2016))	MGLCM (9 orientations and 1 distance)	165	MLP	97.8%
		25 (BRATS 2013)		98.6%
The proposed algorithm	Bi-MGLCM (17 orientation and 1 distance)	214	LSTM	96.3%
		25 (BRATS 2013)		98.9%

The highest classification accuracy was 96.3 ± 0.1%, and this was achieved by combining the LSTM network and the ANOVA method by taking only 204 related descriptors. Compared to the classification accuracy achieved by Quadratic SVM, Naïve Bayes and KNN, which were 93%, 92.5% and 92.1%, respectively. The statistical properties of tissue who have been extracted through the use of biMGLCM, are very important due to the pathological distinction it makes between patients and other patients, and this is done through the use of T2-w images, especially since most of the tumors present in the brain tissue appear It has a higher density compared to the density found in normal brain tissue. Besides, there is another feature of this method that is due to the fact that it uses a single scan method that is done using the MRI and what is found in T2-w images. While BiMGLCM provides great performance and high accuracy in distinguishing between existing natural and abnormal brain tissue, although this method is computationally expensive and the memory requirements and major defects that exist.

References

Al-Waeli AMH. An Automated System for the Classification and Segmentation of Brain Tumours in Mri Images based on the Modified Grey Level Co-Occurrence Matrix: Salford, UK: University of Salford 2017.

Ardekani BA, Kershaw J, Braun M, Kanuo I. Automatic detection of the mid-sagittal plane in 3-D brain images. *IEEE transactions on medical imaging* 1997; 16(6): 947-952.

Bauer S. Medical image analysis and image-based modeling for brain tumor studies. *Verlag nicht ermittelbar* 2013.

Bergo FP, Falcão AX, Yasuda CL, Ruppert GC. Fast, accurate and precise mid-sagittal plane location in 3D MR images of the brain. *In International Joint Conference on Biomedical Engineering Systems and Technologies*, *Springer, Berlin, Heidelberg* 2008: 278-290.

Birry RAK. *Automated classification in digital images of osteogenic differentiated stem cells.* University of Salford 2013.

Gómez W, Pereira WCA, Infantosi AFC. Analysis of co-occurrence texture statistics as a function of gray-level quantization for classifying breast ultrasound. *IEEE transactions on medical imaging* 2012; 31(10): 1889-1899.

Hasan AM, Meziane F. Automated screening of MRI brain scanning using grey level statistics. *Computers & Electrical Engineering* 2016; 53: 276-291.

Hu Q, Nowinski WL. A rapid algorithm for robust and automatic extraction of the midsagittal plane of the human cerebrum from neuroimages based on local symmetry and outlier removal. *NeuroImage* 2003; 20(4): 2153-2165.

Jalab HA, Hasan A. Magnetic Resonance Imaging Segmentation Techniques of Brain Tumors: A Review. *Arch Neurosci* 2019: *e84920*.

Jayalakshmi T, Santhakumaran A. Statistical normalization and back propagation for classification. *International Journal of Computer Theory and Engineering* 2011; 3(1): 1793-8201.

Jayasuriya SA, Liew AWC. Symmetry plane detection in neuroimages based on intensity profile analysis. *In IEEE*

International Symposium on Information Technologies in Medicine and Education 2012; 2: 599-603.

Johnson KJ, Synovec RE. Pattern recognition of jet fuels: comprehensive GC× GC with ANOVA-based feature selection and principal component analysis. *Chemometrics and Intelligent Laboratory Systems* 2002; 60(1-2): 225-237.

Lahmiri S, Boukadoum M. Hybrid discrete wavelet transform and Gabor filter banks processing for features extraction from biomedical images. *Journal of medical engineering* 2013.

https://doi.org/10.1155/2013/104684

Larose DT, Larose CD. *Discovering knowledge in data: an introduction to data mining.* John Wiley & Sons 2014.

Liu Y, Collins RT, Rothfus WE. Automatic bilateral symmetry (midsagittal) plane extraction from pathological 3D neuroradiological images. *In Medical Imaging 1998: Image Processing*, *International Society for Optics and Photonics* 1998; 3338: 1528-1539.

Menze BH, Jakab A, Bauer S, Kalpathy-Cramer J, Farahani K, Kirby J, Wiest R. The multimodal brain tumor image segmentation benchmark (BRATS). *IEEE transactions on medical imaging* 2014; 34(10): 1993-2024.

Nabizadeh N. *Automated brain lesion detection and segmentation using magnetic resonance images.* University of Miami 2015.

Nabizadeh N, Kubat M. Brain tumors detection and segmentation in MR images: Gabor wavelet vs. statistical features. *Computers & Electrical Engineering* 2015; 45: 286-301.

Pantelis G. *Computer Assisted Diagnosis of Brain Tumors based on Statistical Methods and Pattern Recognition Techniques.* PhD, Interdepartmental Postgraduate Program in Medical Physics, University of Patras, Greece 2010.

Ruppert GC, Teverovskiy L, Yu CP, Falcao AX, Liu Y. A new symmetry-based method for mid-sagittal plane extraction in neuroimages. *In IEEE international symposium on biomedical imaging: from nano to macro* 2011: 285-288.

Sachdeva J, Kumar V, Gupta I, Khandelwal N, Ahuja CK. A package-SFERCB- Segmentation, feature extraction, reduction and classification analysis by both SVM and ANN for brain tumors. *Applied soft computing* 2016; 47: 151-167.

Shree NV, Kumar T. Identification and classification of brain tumor MRI images with feature extraction using DWT and probabilistic neural network. *Brain informatics* 2018; 5(1): 23-30.

Singh A. Detection of brain tumor in MRI images, using combination of fuzzy c-means and SVM. *In IEEE 2nd International Conference on Signal Processing and Integrated Networks (SPIN)* 2015: 98-102.

Zulpe N, Pawar V. GLCM textural features for brain tumor classification. *International Journal of Computer Science Issues (IJCSI)* 2012; 9(3): 354-359.

Song D. Subjective universe. *NeuroQuantology,* 2019; 17(6): 65-70. http://doi.org/10.14704/nq.2019.17.6.2428

Heravi MAY, Maghooli K, Rahatabad FN, Rezaee R. Intra-spinal stimulation leads to activation of motor modules and restoration of monitored movements in spinally-injured rabbits. *NeuroQuantology* 2019; 17(6): 71-79.

http://doi.org/10.14704/nq.2019.17.6.2456